Analysis of $\Lambda_b \to \Lambda \ell^+ \ell^-$ transition in SM4 using form factors from Full QCD

K. Azizi[‡],N. Katırcı[†]

Physics Department, Doğuş University, Acıbadem-Kadıköy,

34722 Istanbul, Turkey

[‡]e-mail:kazizi@dogus.edu.tr

[†]e-mail:nkatirci@dogus.edu.tr

Using the responsible form factors calculated via full QCD, we analyze the $\Lambda_b \to \Lambda \ell^+ \ell^-$ transition in the standard model containing fourth generation quarks (SM4). We discuss effects of the presence of t' fourth family quark on related observables like branching ratio, forward-backward asymmetry, baryon polarization as well as double lepton polarization asymmetries. We also compare our results with those obtained in the SM as well as with predictions of the SM4 but using form factors calculated within heavy quark effective theory. The obtained results on branching ratio indicate that the $\Lambda_b \to \Lambda \ell^+ \ell^-$ transition is more probable in full QCD comparing to the heavy quark effective theory. It is also shown that the results on all considered observables in SM4 deviate considerably from the SM predictions when $m_{t'} \geq 400\ GeV$.

PACS numbers: 12.60-i, 13.30.-a, 13.30.Ce, 14.20.Mr

I. INTRODUCTION

The standard model (SM) has been the pillar of particle physics for many years. However, there are some unsolved problems such as the origin of mass, the strong CP problem, neutrino oscillations, origins of dark matter and dark energy, number of generations, matter-antimatter asymmetry, quantum gravity, unification and so on which can not be explained by the SM. To cure such deficiencies, there exist various extensions of the standard model through supersymmetry, SM with fourth generation, etc. or entirely novel explanations, such as string theory, M-theory and extra dimensions.

The new theories beyond the SM need to be confirmed in the experiments. Hence, calculation of many parameters related to the decays of hadrons via new theories such as SM4 are important as they could be studied at particle colliders. It is expected that the LHC will provide possibility to study properties of hadrons as well as their electromagnetic, weak and strong decays. Among these decays, the weak decays of hadrons can play a crucial role in searching for physics beyond the SM. The loop level semileptonic weak transitions of the heavy baryons containing single heavy quark to light baryons induced by the flavor changing neutral currents (FCNC) are useful tools in this respect. In this connection, we analyze the $\Lambda_b \to \Lambda \ell^+ \ell^-$ transition in SM4 by calculating various related parameters like branching ratio, forward-backward asymmetry, baryon polarization as well as double lepton polarization asymmetries. Here, we use all involved twelve form factors recently calculated in full QCD [1]. This work is an extension of the previous works [2–4] where the two form factors calculated within heavy quark effective theory (HQET) are used.

In the SM, the $\Lambda_b \to \Lambda \ell^+ \ell^-$ channel proceeds via FCNC transition of $b \to s \ell^+ \ell^-$ at quark level. The latter is described via a low energy effective Hamiltonian containing Wilson coefficients. In SM4, the form of Hamiltonian does not change but due to additional interactions of the fourth family quark t' with other particles the Wilson coefficients are modified. Hence,

$$\begin{aligned}
C_7^{eff,tot}(m_{t'}, r_{sb}, \phi_{sb}) &= C_7^{eff,SM} + \frac{\lambda_{t'}(r_{sb}, \phi_{sb})}{\lambda_t} C_7^{eff,new}(m_{t'}) \ , \\
C_9^{eff,tot}(m_{t'}, r_{sb}, \phi_{sb}) &= C_9^{eff,SM} + \frac{\lambda_{t'}(r_{sb}, \phi_{sb})}{\lambda_t} C_9^{eff,new}(m_{t'}) \ , \\
C_{10}^{tot}(m_{t'}, r_{sb}, \phi_{sb}) &= C_{10}^{SM} + \frac{\lambda_{t'}(r_{sb}, \phi_{sb})}{\lambda_t} C_{10}^{new}(m_{t'}) \ ,
\end{aligned} \tag{1}$$

where

$$\lambda_t = V_{tb} V_{ts}^* \qquad \text{and} \qquad \lambda_{t'}(r_{sb}, \phi_{sb}) = V_{t'b} V_{t's}^* = r_{sb} e^{i\phi_{sb}}. \tag{2}$$

Here, V_{tb}, V_{ts} are elements of Cabibbo-Kobayashi-Maskawa (CKM) matrix in the SM and $V_{t'b}$, $V_{t's}$ are elements of the CKM matrix in the SM4. In the above relations, ($m_{t'}$, r_{sb}, ϕ_{sb}

) is a set of fourth generation parameters which we are going to discuss the sensitivity of physical observables to them. The new Wilson coefficients, $C_7^{eff,new}(m_{t'}), C_9^{eff,new}(m_{t'})$ and $C_{10}^{new}(m_{t'})$ in Eqs. (1) are obtained by replacing the mass of top quark by its SM4 version ($m_t \to m_{t'}$) [5, 6].

It is expected that the masses of the fourth generation quarks are in the interval (400-600) GeV [7]. As the mass difference between these two quarks is small, we will refer to both members of the fourth family by t'. For the recent status of the SM4 quarks see for instance [8–10] and references therein.

The outline of the paper is as follows. In next section, we present the effective Hamiltonian and transition matrix elements describing the decay under consideration. In section III, we present the explicit expressions for physical observables such as differential decay rate, forward backward asymmetry, baryon polarization and double lepton polarization asymmetries. This section also encompass our numerical analysis on the physical quantities under study as well as our discussions. Finally, we will have a concluding section.

II. THE $\Lambda_b \to \Lambda \ell^+ \ell^-$ TRANSITION

A. The Effective Hamiltonian

The quark structures of the initial and final baryons in $\Lambda_b \to \Lambda \ell^+ \ell^-$ indicate that this channel proceeds via FCNC transition of $b \to s \ell^+ \ell^-$, whose effective Hamiltonian in the SM is written as

$$\mathcal{H}^{eff} = \frac{G_F \alpha_{em} V_{tb} V_{ts}^*}{2\sqrt{2}\pi} \Big[C_9^{eff} \bar{s}\gamma_\mu (1-\gamma_5) b\, \bar{\ell}\gamma^\mu \ell + C_{10} \bar{s}\gamma_\mu (1-\gamma_5) b\, \bar{\ell}\gamma^\mu \gamma_5 \ell - 2 m_b C_7^{eff} \frac{1}{q^2} \bar{s} i\sigma_{\mu\nu} q^\nu (1+\gamma_5) b\, \bar{\ell}\gamma^\mu \ell \Big] , \tag{3}$$

where G_F is the Fermi constant, α_{em} is the fine structure constant at Z mass scale, and as we previously mentioned the C_7^{eff}, C_9^{eff} and C_{10} are the Wilson coefficients representing different interactions. In the following, we present the explicit expressions of the Wilson coefficients in the SM. To get their expressions in SM4, it is enough to apply Eq. (1).

The C_7^{eff} is given as [5, 11, 12]

$$C_7^{eff} = \eta^{\frac{16}{23}} C_7(\mu_W) + \frac{8}{3}\left(\eta^{\frac{14}{23}} - \eta^{\frac{16}{23}}\right) C_8(\mu_W) + C_2(\mu_W) \sum_{i=1}^{8} h_i \eta^{a_i} , \tag{4}$$

where

$$\eta = \frac{\alpha_s(\mu_W)}{\alpha_s(\mu_b)} , \quad \text{and} \quad \alpha_s(x) = \frac{\alpha_s(m_Z)}{1 - \beta_0 \frac{\alpha_s(m_Z)}{2\pi} \ln(\frac{m_Z}{x})}, \tag{5}$$

with $\alpha_s(m_Z) = 0.118$ and $\beta_0 = \frac{23}{3}$. The coefficients a_i and h_i are given as [5, 12]:

$$\begin{aligned} a_i &= (\quad \tfrac{14}{23}, \quad \tfrac{16}{23}, \ \tfrac{6}{23}, \ -\tfrac{12}{23}, \quad 0.4086, \ -0.4230, \ -0.8994, \quad 0.1456\,), \\ h_i &= (\,2.2996, \ -1.0880, \ -\tfrac{3}{7}, \ -\tfrac{1}{14}, \ -0.6494, \ -0.0380, \ -0.0186, \ -0.0057\,). \end{aligned} \tag{6}$$

The functions $C_2(\mu_W)$, $C_7(\mu_W)$ and $C_8(\mu_W)$ inside the C_7^{eff} are given as:

$$C_2(\mu_W) = 1, \quad C_7(\mu_W) = -\frac{1}{2}D_0(x_t)\ , \quad C_8(\mu_W) = -\frac{1}{2}E_0(x_t) \tag{7}$$

where $x_t = \frac{m_t^2}{m_W^2}$ and

$$D_0(x_t) = -\frac{(8x_t^3 + 5x_t^2 - 7x_t)}{12(1-x_t^3)} + \frac{x_t^2(2-3x_t)}{2(1-x_t)^4}\ln x_t\ , \tag{8}$$

$$E_0(x_t) = -\frac{x_t(x_t^2 - 5x_t - 2)}{4(1-x_t^3)} + \frac{3x_t^2}{2(1-x_t)^4}\ln x_t\ . \tag{9}$$

The Wilson coefficient C_{10} is given by

$$C_{10} = -\frac{Y(x_t)}{\sin^2\theta_W} \tag{10}$$

where $\sin^2\theta_W = 0.23$ and

$$Y(x_t) = \frac{x_t}{8}\left[\frac{x_t - 4}{x_t - 1} + \frac{3x_t}{(x_t-1)^2}\ln x_t\right]\ . \tag{11}$$

In leading log approximation, the Wilson coefficient $C_9^{eff}(s')$ entering the effective Hamiltonian of the channel under consideration can be written as [5, 12]:

$$\begin{aligned} C_9^{eff}(\hat{s}') = {} & C_9\eta(\hat{s}') + h(z,\hat{s}')\,(3C_1 + C_2 + 3C_3 + C_4 + 3C_5 + C_6) \\ & -\frac{1}{2}h(1,\hat{s}')\,(4C_3 + 4C_4 + 3C_5 + C_6) \\ & -\frac{1}{2}h(0,\hat{s}')\,(C_3 + 3C_4) + \frac{2}{9}\,(3C_3 + C_4 + 3C_5 + C_6) \end{aligned} \tag{12}$$

where

$$\eta(\hat{s}') = 1 + \frac{\alpha_s(\mu_b)}{\pi}\,\omega(\hat{s}'), \tag{13}$$

$$\begin{aligned} \omega(\hat{s}') = {} & -\frac{2}{9}\pi^2 - \frac{4}{3}\mathrm{Li}_2(\hat{s}') - \frac{2}{3}\ln\hat{s}'\ln(1-\hat{s}') - \frac{5+4\hat{s}'}{3(1+2\hat{s}')}\ln(1-\hat{s}') - \\ & \frac{2\hat{s}'(1+\hat{s}')(1-2\hat{s}')}{3(1-\hat{s}')^2(1+2\hat{s}')}\ln\hat{s}' + \frac{5+9\hat{s}'-6\hat{s}'^2}{6(1-\hat{s}')(1+2\hat{s}')}, \end{aligned} \tag{14}$$

with $\hat{s}' = \frac{q^2}{m_b^2}$. The allowed region for the transferred momentum square, q^2 is $4m_l^2 \leq q^2 \leq (m_{\Lambda_b} - m_\Lambda)^2$. The C_9 is given as

$$C_9 = P_0^{NDR} + \frac{Y(x_t)}{\sin^2\theta_W} - 4Z(x_t), \tag{15}$$

where $P_0^{NDR} = 2.60 \pm 0.25$ [5, 12] in the naive dimensional regularization scheme.

The function, $Z(x_t)$ is defined as:

$$Z(x_t) = \frac{18(x_t)^4 - 163x_t^3 + 259x_t^2 - 108x_t}{144(x_t-1)^3}\left[\frac{32(x_t)^4 - 38x_t^3 - 15x_t^2 + 18x_t}{72(x_t-1)^4} - \frac{1}{9}\right]\ln x_t. \tag{16}$$

The remaining coefficients in Eq. (12) is defined as:

$$C_j = \sum_{i=1}^{8} k_{ji}\eta^{a_i} \qquad (j = 1, ...6) \tag{17}$$

where k_{ji} are given as:

$$\begin{aligned}
k_{1i} &= (\,0,\ 0,\ \ \tfrac{1}{2},\ -\tfrac{1}{2},\ \ \ 0,\ \ \ \ 0,\ \ \ \ 0,\ \ \ \ 0\,),\\
k_{2i} &= (\,0,\ 0,\ \ \tfrac{1}{2},\ \ \tfrac{1}{2},\ \ \ 0,\ \ \ \ 0,\ \ \ \ 0,\ \ \ \ 0\,),\\
k_{3i} &= (\,0,\ 0,\ -\tfrac{1}{14},\ \ \tfrac{1}{6},\ \ 0.0510,\ -0.1403,\ -0.0113,\ \ 0.0054\,),\\
k_{4i} &= (\,0,\ 0,\ -\tfrac{1}{14},\ -\tfrac{1}{6},\ \ 0.0984,\ \ 0.1214,\ \ 0.0156,\ \ 0.0026\,),\\
k_{5i} &= (\,0,\ 0,\ \ \ 0,\ \ \ 0,\ -0.0397,\ \ 0.0117,\ -0.0025,\ \ 0.0304\,),\\
k_{6i} &= (\,0,\ 0,\ \ \ 0,\ \ \ 0,\ \ 0.0335,\ \ 0.0239,\ -0.0462,\ -0.0112\,).
\end{aligned} \tag{18}$$

Finally, the $h(y, \hat{s}')$ function has the following explicit expression:

$$h(y,\hat{s}') = -\frac{8}{9}\ln\frac{m_b}{\mu_b} - \frac{8}{9}\ln y + \frac{8}{27} + \frac{4}{9}x \tag{19}$$

$$-\frac{2}{9}(2+x)|1-x|^{1/2}\begin{cases}\left(\ln\left|\frac{\sqrt{1-x}+1}{\sqrt{1-x}-1}\right| - i\pi\right), & \text{for } x \equiv \frac{4z^2}{\hat{s}'} < 1\\ 2\arctan\frac{1}{\sqrt{x-1}}, & \text{for } x \equiv \frac{4z^2}{\hat{s}'} > 1,\end{cases} \tag{20}$$

where $y = 1$ or $y = z = \frac{m_c}{m_b}$ and,

$$h(0,\hat{s}') = \frac{8}{27} - \frac{8}{9}\ln\frac{m_b}{\mu_b} - \frac{4}{9}\ln\hat{s}' + \frac{4}{9}i\pi. \tag{21}$$

B. Transition Matrix Elements and Form Factors

The transition matrix elements for $\Lambda_b \to \Lambda\ell^+\ell^-$ are obtained by sandwiching the effective Hamiltonian between the initial and final baryonic states. These matrix elements are parametrized in terms of twelve form factors in full QCD in the following way:

$$\begin{aligned}
\langle\Lambda(p) \mid \bar{s}\gamma_\mu(1-\gamma_5)b \mid \Lambda_b(p+q)\rangle = \bar{u}_\Lambda(p)\Big[&\gamma_\mu f_1(q^2) + i\sigma_{\mu\nu}q^\nu f_2(q^2) + q^\mu f_3(q^2)\\
&-\gamma_\mu\gamma_5 g_1(q^2) - i\sigma_{\mu\nu}\gamma_5 q^\nu g_2(q^2) - q^\mu\gamma_5 g_3(q^2)\Big]u_{\Lambda_b}(p+q)\ ,
\end{aligned} \tag{22}$$

$$\langle \Lambda(p) \mid \bar{s} i\sigma_{\mu\nu} q^\nu (1+\gamma_5) b \mid \Lambda_b(p+q)\rangle = \bar{u}_\Lambda(p)\Big[\gamma_\mu f_1^T(q^2) + i\sigma_{\mu\nu}q^\nu f_2^T(q^2) + q^\mu f_3^T(q^2) + \gamma_\mu\gamma_5 g_1^T(q^2) + i\sigma_{\mu\nu}\gamma_5 q^\nu g_2^T(q^2) + q^\mu\gamma_5 g_3^T(q^2)\Big] u_{\Lambda_b}(p+q) \ , \tag{23}$$

where f_1, f_2, f_3, g_1, g_2, g_3, f_1^T, f_2^T, f_3^T, g_1^T, g_2^T and g_3^T are transition form factors in full theory. These form factors have been recently calculated in [1] in the framework of light cone QCD sum rules.

In the HQET, the twelve form factors in full QCD reduce to two form factors, F_1 and F_2, hence the transition matrix element in this limit is defined as [13, 14]:

$$\langle \Lambda(p) \mid \bar{s}\Gamma b \mid \Lambda_b(p+q)\rangle = \bar{u}_\Lambda(p)[F_1(q^2) + \not{v} F_2(q^2)]\Gamma u_{\Lambda_b}(p+q), \tag{24}$$

where Γ denotes any Dirac matrices and $\not{v} = (\not{p} + \not{q})/m_{\Lambda_b}$. These form factor are calculated in [15]. Comparing the definitions of the transition matrix elements both in full QCD and HQET theories, one can easily find the following relations among the above mentioned form factors:

$$\begin{aligned}
f_1 &= g_1 = f_2^T = g_2^T = F_1 + \frac{m_\Lambda}{m_{\Lambda_b}} F_2 \ , \\
f_2 &= g_2 = f_3 = g_3 = \frac{F_2}{m_{\Lambda_b}} \ , \\
f_1^T &= g_1^T = \frac{F_2}{m_{\Lambda_b}} q^2 \ , \\
f_3^T &= -\frac{F_2}{m_{\Lambda_b}}(m_{\Lambda_b} - m_\Lambda) \ , \\
g_3^T &= \frac{F_2}{m_{\Lambda_b}}(m_{\Lambda_b} + m_\Lambda) \ .
\end{aligned} \tag{25}$$

III. PHYSICAL OBSERVABLES CHARACTERIZING THE $\Lambda_b \to \Lambda \ell^+ \ell^-$ TRANSITION

A. Branching Ratio

Using the decay amplitude and transition matrix elements in terms of form factors, the differential decay rate is obtained as a function of SM4 parameters as [16–18]:

$$\frac{d\Gamma}{d\hat{s}dz}(z, \hat{s}, m_{t'}, r_{sb}, \phi_{sb}) = \frac{G_F^2 \alpha_{em}^2 m_{\Lambda_b}}{16382\pi^5} |V_{tb}V_{ts}^*|^2 v\sqrt{\lambda}\Big[\mathcal{T}_0(\hat{s}, m_{t'}, r_{sb}, \phi_{sb}) + \mathcal{T}_1(\hat{s}, m_{t'}, r_{sb}, \phi_{sb}) z + \mathcal{T}_2(\hat{s}, m_{t'}, r_{sb}, \phi_{sb}) z^2\Big] \ , \tag{26}$$

where $z = \cos\theta$ with θ being the angle between the momenta of Λ_b and ℓ^- in the center of mass of leptons, $\lambda = \lambda(1, r, \hat{s}) = 1 + r^2 + \hat{s}^2 - 2r - 2\hat{s} - 2r\hat{s}$, $r = m_\Lambda^2/m_{\Lambda_b}^2$ and $v = \sqrt{1 - \frac{4m_\ell^2}{q^2}}$. Here, $\hat{s} = \frac{q^2}{m_{\Lambda_b}^2}$ and we have the relation, $\hat{s}' = \frac{\hat{s} m_{\Lambda_b}^2}{m_b^2}$ between the $\hat{s}$ and previously used $\hat{s}'$. The functions, $\mathcal{T}_0(\hat{s}, m_{t'}, r_{sb}, \phi_{sb})$, $\mathcal{T}_1(\hat{s}, m_{t'}, r_{sb}, \phi_{sb})$ and $\mathcal{T}_2(\hat{s}, m_{t'}, r_{sb}, \phi_{sb})$ are given as (see also [1]):

$$
\begin{aligned}
\mathcal{T}_0(\hat{s}, m_{t'}, r_{sb}, \phi_{sb}) &= 32 m_\ell^2 m_{\Lambda_b}^4 \hat{s}(1 + r - \hat{s}) \Big(|D_3|^2 + |E_3|^2 \Big) \\
&+ 64 m_\ell^2 m_{\Lambda_b}^3 (1 - r - \hat{s})\, \mathrm{Re}[D_1^* E_3 + D_3 E_1^*] \\
&+ 64 m_{\Lambda_b}^2 \sqrt{r} (6 m_\ell^2 - m_{\Lambda_b}^2 \hat{s}) \mathrm{Re}[D_1^* E_1] \\
&+ 64 m_\ell^2 m_{\Lambda_b}^3 \sqrt{r} \Big(2 m_{\Lambda_b} \hat{s} \mathrm{Re}[D_3^* E_3] + (1 - r + \hat{s}) \mathrm{Re}[D_1^* D_3 + E_1^* E_3] \Big) \\
&+ 32 m_{\Lambda_b}^2 (2 m_\ell^2 + m_{\Lambda_b}^2 \hat{s}) \Big\{ (1 - r + \hat{s}) m_{\Lambda_b} \sqrt{r}\, \mathrm{Re}[A_1^* A_2 + B_1^* B_2] \\
&- m_{\Lambda_b} (1 - r - \hat{s})\, \mathrm{Re}[A_1^* B_2 + A_2^* B_1] - 2\sqrt{r} \Big(\mathrm{Re}[A_1^* B_1] + m_{\Lambda_b}^2 \hat{s}\, \mathrm{Re}[A_2^* B_2] \Big) \Big\} \\
&+ 8 m_{\Lambda_b}^2 \Big\{ 4 m_\ell^2 (1 + r - \hat{s}) + m_{\Lambda_b}^2 \Big[(1 - r)^2 - \hat{s}^2 \Big] \Big\} \Big(|A_1|^2 + |B_1|^2 \Big) \\
&+ 8 m_{\Lambda_b}^4 \Big\{ 4 m_\ell^2 \Big[\lambda + (1 + r - \hat{s}) \hat{s} \Big] + m_{\Lambda_b}^2 \hat{s} \Big[(1 - r)^2 - \hat{s}^2 \Big] \Big\} \Big(|A_2|^2 + |B_2|^2 \Big) \\
&- 8 m_{\Lambda_b}^2 \Big\{ 4 m_\ell^2 (1 + r - \hat{s}) - m_{\Lambda_b}^2 \Big[(1 - r)^2 - \hat{s}^2 \Big] \Big\} \Big(|D_1|^2 + |E_1|^2 \Big) \\
&+ 8 m_{\Lambda_b}^5 \hat{s} v^2 \Big\{ - 8 m_{\Lambda_b} \hat{s} \sqrt{r}\, \mathrm{Re}[D_2^* E_2] + 4(1 - r + \hat{s}) \sqrt{r}\, \mathrm{Re}[D_1^* D_2 + E_1^* E_2] \\
&- 4(1 - r - \hat{s})\, \mathrm{Re}[D_1^* E_2 + D_2^* E_1] + m_{\Lambda_b} \Big[(1 - r)^2 - \hat{s}^2 \Big] \Big(|D_2|^2 + |E_2|^2 \Big) \Big\},
\end{aligned}
\tag{27}
$$

$$
\begin{aligned}
\mathcal{T}_1(\hat{s}, m_{t'}, r_{sb}, \phi_{sb}) &= -16 m_{\Lambda_b}^4 \hat{s} v \sqrt{\lambda} \Big\{ 2Re(A_1^* D_1) - 2Re(B_1^* E_1) \\
&+ 2 m_{\Lambda_b} Re(B_1^* D_2 - B_2^* D_1 + A_2^* E_1 - A_1^* E_2) \Big\} \\
&+ 32 m_{\Lambda_b}^5 \hat{s}\ v \sqrt{\lambda} \Big\{ m_{\Lambda_b} (1 - r) Re(A_2^* D_2 - B_2^* E_2) \\
&+ \sqrt{r} Re(A_2^* D_1 + A_1^* D_2 - B_2^* E_1 - B_1^* E_2) \Big\}\,,
\end{aligned}
\tag{28}
$$

$$
\begin{aligned}
\mathcal{T}_2(\hat{s}, m_{t'}, r_{sb}, \phi_{sb}) &= -8 m_{\Lambda_b}^4 v^2 \lambda \Big(|A_1|^2 + |B_1|^2 + |D_1|^2 + |E_1|^2 \Big) \\
&+ 8 m_{\Lambda_b}^6 \hat{s} v^2 \lambda \Big(|A_2|^2 + |B_2|^2 + |D_2|^2 + |E_2|^2 \Big)\,,
\end{aligned}
\tag{29}
$$

where,

$$
\begin{aligned}
A_1 &= A_1(\hat{s}, m_{t'}, r_{sb}, \phi_{sb}) \\
&= \frac{1}{\hat{s} m_{\Lambda_b}^2} \Big(f_1^T(\hat{s}) + g_1^T(\hat{s}) \Big) \Big(-2 m_b C_7^{eff}(\hat{s}, m_{t'}, r_{sb}, \phi_{sb}) \Big) + \Big(f_1(\hat{s}) - g_1(\hat{s}) \Big) C_9^{eff}(\hat{s}, m_{t'}, r_{sb}, \phi_{sb}) \\
A_2 &= A_1\,(1 \to 2)\ , \\
A_3 &= A_1\,(1 \to 3)\ , \\
B_1 &= A_1 \Big(g_1(\hat{s}) \to -g_1(\hat{s});\ g_1^T(\hat{s}) \to -g_1^T(\hat{s}) \Big)\ , \\
B_2 &= B_1\,(1 \to 2)\ ,
\end{aligned}
$$

$$
\begin{aligned}
B_3 &= B_1\,(1\to 3)\ , \\
D_1 &= \Big(f_1(\hat{s}) - g_1(\hat{s})\Big) C_{10}(\hat{s}, m_{t'}, r_{sb}, \phi_{sb})\ , \\
D_2 &= D_1\,(1\to 2)\ , \\
D_3 &= D_1\,(1\to 3)\ , \\
E_1 &= D_1\Big(g_1(\hat{s}) \to -g_1(\hat{s})\Big)\ , \\
E_2 &= E_1\,(1\to 2)\ , \\
E_3 &= E_1\,(1\to 3)\ .
\end{aligned} \tag{30}
$$

Integrating the aforementioned angular dependent differential decay rate over z, we get the $\hat{s}$ and SM4 parameters dependent differential decay width as

$$
\frac{d\Gamma(\hat{s}, m_{t'}, r_{sb}, \phi_{sb})}{d\hat{s}} = \frac{G_F^2 \alpha_{em}^2 m_{\Lambda_b}}{8192\pi^5} |V_{tb}V_{ts}^*|^2 v\sqrt{\lambda}\, \Delta(\hat{s}, m_{t'}, r_{sb}, \phi_{sb})\ , \tag{31}
$$

where,

$$
\Delta(\hat{s}, m_{t'}, r_{sb}, \phi_{sb}) = \mathcal{T}_0(\hat{s}, m_{t'}, r_{sb}, \phi_{sb}) + \frac{1}{3}\mathcal{T}_2(\hat{s}, m_{t'}, r_{sb}, \phi_{sb}). \tag{32}
$$

Performing integration over $\hat{s}$ in the kinematical region $\frac{4m_\ell^2}{m_{\Lambda_b}^2} \leq \hat{s} \leq (1-\sqrt{r})^2$, the total decay width is obtained. Finally, using the lifetime of the Λ_b baryon, we obtain the branching ratio depending on SM4 parameters.

In further numerical analysis, we take the values, $m_t = 167\ GeV$, $m_W = 80.4\ GeV$, $m_b = 4.8\ GeV$, $m_c = 1.35\ GeV$, $\mu_b = 5\ GeV$, $\mu_W = 80.4\ GeV$, $m_e = 0.00051$, $m_\tau = 1.778$, $m_\mu = 0.105\ GeV$, $|V_{tb}V_{ts}^*| = 0.041$, $G_F = 1.166 \times 10^{-5}\ GeV^{-2}$, $\alpha_{em} = \frac{1}{129}$, $\tau_{\Lambda_b} = 1.383 \times 10^{-12}\ s$, $m_\Lambda = 1.116\ GeV$ and $m_{\Lambda_b} = 5.624\ GeV$. The present SM measurements and unitarity condition of the CKM matrix imply that [19–22]

$$
r_{sb} = |V_{t'b}V_{t's}^*| \leq 1.5 \times 10^{-2}. \tag{33}
$$

In our numerical calculations, we will consider the three different values $r_{sb} = |V_{t'b}V_{t's}^*| = 0.005,\ 0.010$ and 0.015. As we previously mentioned, the masses of the fourth generation quarks are expected to be in the interval (400-600) GeV. In the present work, we will plot our figures considering the $m_{t'}$ in the interval (175-600) GeV to see better at which points the SM4 results start to deviate from the usual SM predictions. The ϕ_{sb} is taken as $\phi_{sb} = \frac{\pi}{2}$ [23] (see also [24]).

The dependence of the branching ratio of the channel under consideration for the μ and τ leptons on $m_{t'}$ at three fixed values of the r_{sb} as well as the SM are presented in figures 1 and 2. In these figures, the left graph corresponds to the HQET while the graph on the right refers to the full QCD. We take into account the errors of the form factors in our analysis, hence we have a bound for each SM and SM4 with three different values of the r_{sb} obtained from adding (subtracting) of the uncertainties to (from) the central values.

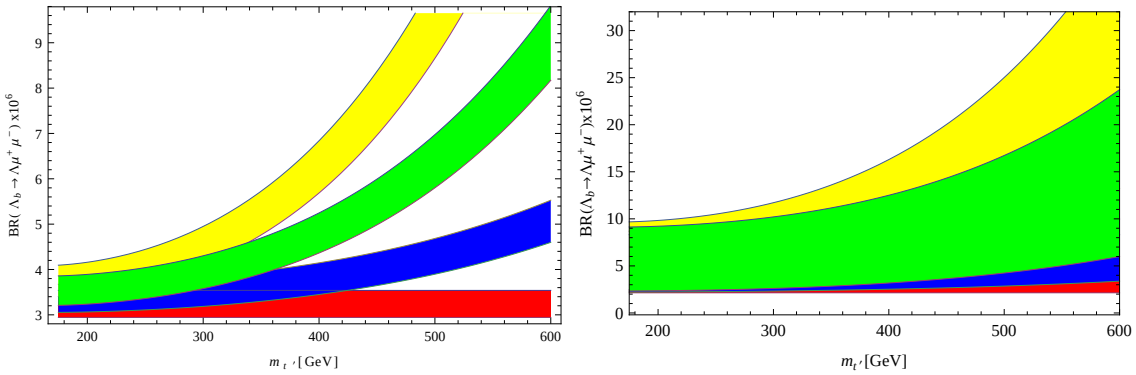

FIG. 1. The dependence of branching ratio for the $\Lambda_b \to \Lambda\mu^+\mu^-$ decay on $m_{t'}$. The red band corresponds to the SM, while the blue, green and yellow bands belong to the SM4 for $r_{sb} = 0.005,\ 0.01$ and 0.015, respectively. The left graph corresponds to the HQET while the graph on the right refers to the full QCD.

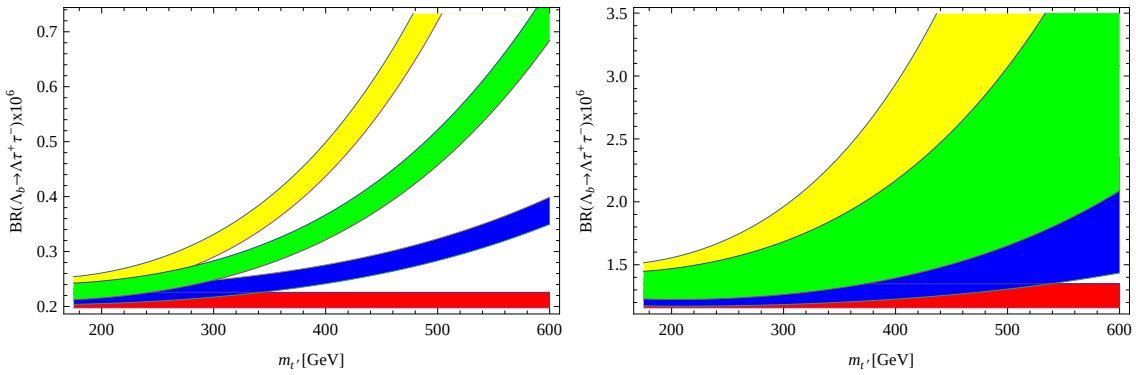

FIG. 2. The same as FIG. 1 but for τ.

From these figures, we see that

- in all cases, the branching ratios in SM4 grow increasing the fourth generation quark mass. The deviation of the SM4 results from those of the SM becomes important at $m_{t'} \simeq 400\ GeV$ and our results favor $m_{t'} \geq 400\ GeV$. This is in good consistency with the results of [7] in explanation of the observed CP asymmetries in the B and B_s decays.

- Increasing in the r_{sb} leads to an increase in the value of the branching ratio in all cases. The maximum deviation of the SM4 results from those of the SM belong to the $r_{sb} = 0.015$ at any fixed values of the $m_{t'}$ in the interval $400\ GeV \leq m_{t'} \leq 600\ GeV$. As far as the branching ratio is concerned, the difference between the SM and SM4 results with $r_{sb} = 0.005$ is considerable in HQET approximation but the uncertainties of the form factors approximately kill this difference in full theory. For $r_{sb} \in [0.1 - 0.15]$ the deviation of the SM4 results from those of the SM cannot be killed by the errors of the form factors in both HQET and Full

theories. Such considerable discrepancy can be considered as an indication for existing the fourth generation of the quarks.

- As it is expected, the branching ratios in τ channel are small compared to the μ channel.

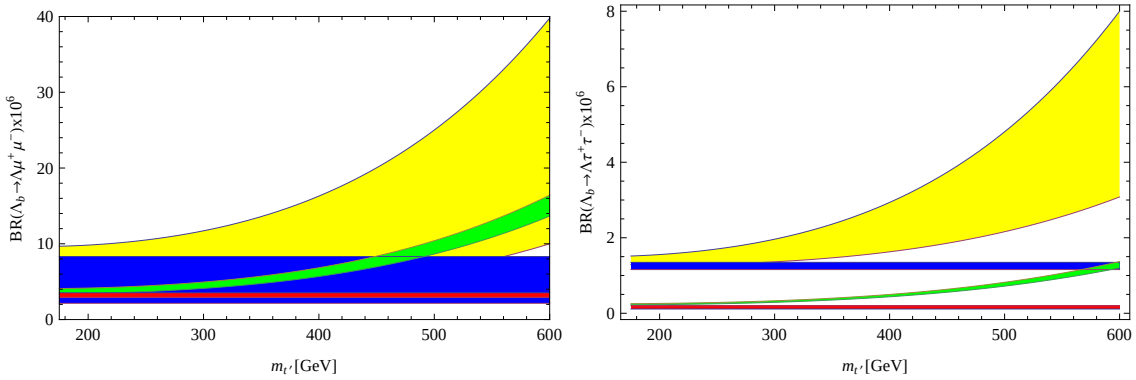

FIG. 3. Comparison of the branching ratio for the $\Lambda_b \to \Lambda l^+ l^-$ decay in full QCD and HQET. The blue and yellow bands respectively correspond to the SM and SM4 ($r_{sb} = 0.015$) in full QCD, while the red and green bands respectively refer to the SM and SM4 ($r_{sb} = 0.015$) in HQET.

We also compare the full QCD and HQET results of the branching ratios obtained from the SM and SM4 with only $r_{sb} = 0.015$ together in figure 3 for both leptons. Looking at this figure, we deduce that

- the full QCD results on branching ratios sweep large areas compared to those of the HQET. As far as the branching ratios are considered, the SM and SM4 with $r_{sb} = 0.015$ bands obtained from the HQET lie inside the bands of the full QCD in μ channel but we see considerable discrepancy between predictions of these theories in the τ channel.

B. Forward-backward asymmetry

The forward-backward asymmetry refers to the difference between the number of particles that move on the forward and those move on the backward direction. It is one of the promising tools in looking for new physics beyond the SM. The SM4 parameters dependent forward-backward asymmetry is defined as:

$$\mathcal{A}_{FB}(\hat{s}, m_{t'}, r_{sb}, \phi_{sb}) = \frac{\displaystyle\int_0^1 \frac{d\Gamma}{d\hat{s}dz}(z, \hat{s}, m_{t'}, r_{sb}, \phi_{sb})\, dz - \int_{-1}^0 \frac{d\Gamma}{d\hat{s}dz}(z, \hat{s}, m_{t'}, r_{sb}, \phi_{sb})\, dz}{\displaystyle\int_0^1 \frac{d\Gamma}{d\hat{s}dz}(z, \hat{s}, m_{t'}, r_{sb}, \phi_{sb})\, dz + \int_{-1}^0 \frac{d\Gamma}{d\hat{s}dz}(z, \hat{s}, m_{t'}, r_{sb}, \phi_{sb})\, dz}. \quad (34)$$

Using the $\hat{s}$, z and fourth family parameters dependent differential decay rate we plot the $\mathcal{A}_{FB}$ in terms of $m_{t'}$ at $\hat{s} = 0.5$ and at three fixed values of the r_{sb} and the SM in figures 4 and 5.

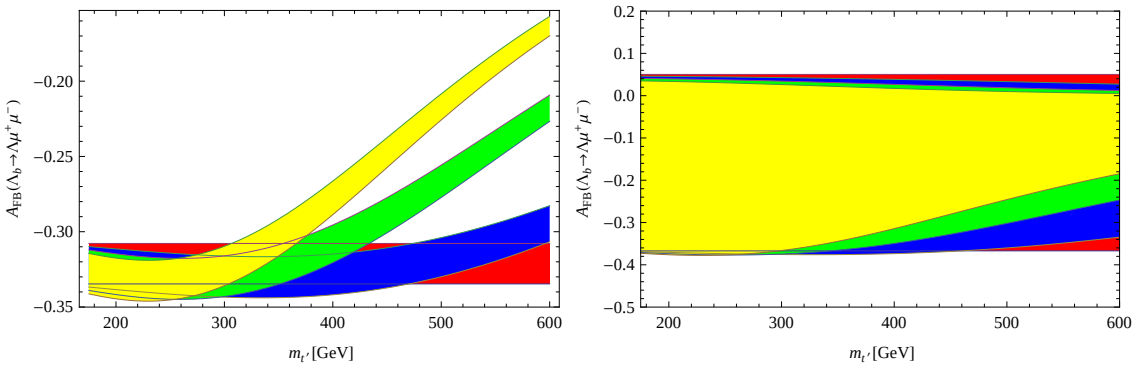

FIG. 4. The dependence of forward-backward asymmetry for the $\Lambda_b \to \Lambda \mu^+ \mu^-$ decay on $m_{t'}$ at $\hat{s} = 0.5$. The red band corresponds to the SM, while the blue, green and yellow bands belong to the SM4 for $r_{sb} = 0.005,\ 0.01$ and 0.015, respectively. The left graph corresponds to the HQET while the graph on the right refers to the full QCD.

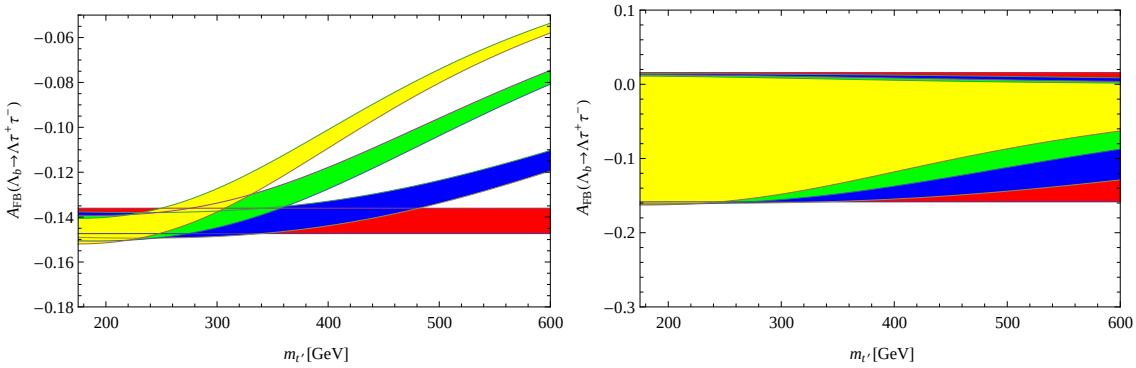

FIG. 5. The same as FIG. 4 but for τ.

From these figures, it is clear that,

- our analysis on the forward-backward asymmetry also seems to favor $m_{t'} \geq 400\ GeV$.

- There is considerable HQET violations in both lepton channels. The difference between the predictions of the full theory and HQET is large in μ channel compared to that of the τ.

- There are considerable discrepancies between the SM4 and the SM results at high $m_{t'}$ values in HQET theory for both leptons. However, the uncertainties of the form factors in full theory suppress these differences such that the results of SM4 for all values of the r_{sb} and $m_{t'}$ lie inside the SM bands.

C. Baryon Polarizations

The definitions for the normal (P_N), longitudinal (P_L) and transversal (P_T) polarizations of the Λ baryon in the massive lepton case, are given in [25]. Using those definitions, the general model independent expressions for the above polarizations are calculated in [26, 27]). In the case of SM4, those expressions reduce to the following explicit forms:

$$
\begin{aligned}
P_N(\hat{s}, m_{t'}, r_{sb}, \phi_{sb}) = & \frac{8\pi m_{\Lambda_b}^3 v\sqrt{\hat{s}}}{\Delta(\hat{s}, m_{t'}, r_{sb}, \phi_{sb})}\Big\{ -2m_{\Lambda_b}(1-r+\hat{s})\sqrt{r}\,\mathrm{Re}[A_1^* D_1 + B_1^* E_1] \\
& + m_{\Lambda_b}(1-\sqrt{r})[(1+\sqrt{r})^2 - \hat{s}]\left(m_\ell \mathrm{Re}[(A_2 - B_2)^* F_1]\right) \\
& + m_\ell[(1+\sqrt{r})^2 - \hat{s}]\,\mathrm{Re}[A_1^* F_1] \\
& + 4m_{\Lambda_b}^2 \hat{s}\sqrt{r}\,\mathrm{Re}[A_1^* E_2 + A_2^* E_1 + B_1^* D_2 + B_2^* D_1] \\
& - 2m_{\Lambda_b}^3 \hat{s}\sqrt{r}(1-r+\hat{s})\,\mathrm{Re}[A_2^* D_2 + B_2^* E_2^*] \\
& + 2m_{\Lambda_b}(1-r-\hat{s})\left(\mathrm{Re}[A_1^* E_1 + B_1^* D_1] + m_{\Lambda_b}^2 \hat{s}\mathrm{Re}[A_2^* E_2 + B_2^* D_2]\right) \\
& - m_{\Lambda_b}^2[(1-r)^2 - \hat{s}^2]\,\mathrm{Re}[A_1^* D_2 + A_2^* D_1 + B_1^* E_2 + B_2^* E_1] \\
& - m_\ell[(1+\sqrt{r})^2 - \hat{s}]\,\mathrm{Re}[B_1^* F_1]\Big\}\,,
\end{aligned} \tag{35}
$$

$$
\begin{aligned}
P_L(\hat{s}, m_{t'}, r_{sb}, \phi_{sb}) = & \frac{16 m_{\Lambda_b}^2\sqrt{\lambda}}{\Delta(\hat{s}, m_{t'}, r_{sb}, \phi_{sb})}\Big\{ 8m_\ell^2 m_{\Lambda_b}\left(\mathrm{Re}[D_1^* E_3 - D_3^* E_1] + \sqrt{r}\mathrm{Re}[D_1^* D_3 - E_1^* E_3)]\right) \\
& + 2m_\ell m_{\Lambda_b}(1+\sqrt{r})\mathrm{Re}[(D_1 - E_1)^* F_2] \\
& - 2m_\ell m_{\Lambda_b}^2 \hat{s}\left\{\mathrm{Re}[(D_3 - E_3)^* F_2] + 2m_\ell(|D_3|^2 - |E_3|^2)\right\} \\
& - 4m_{\Lambda_b}(2m_\ell^2 + m_{\Lambda_b}^2\hat{s})\,\mathrm{Re}[A_1^* B_2 - A_2^* B_1] \\
& - \frac{4}{3}m_{\Lambda_b}^3 \hat{s} v^2\left(3\mathrm{Re}[D_1^* E_2 - D_2^* E_1] + \sqrt{r}\mathrm{Re}[D_1^* D_2 - E_1^* E_2]\right) \\
& - \frac{4}{3}m_{\Lambda_b}\sqrt{r}(6m_\ell^2 + m_{\Lambda_b}^2\hat{s}v^2)\,\mathrm{Re}[A_1^* A_2 - B_1^* B_2] \\
& + \frac{1}{3}\Big\{3[4m_\ell^2 + m_{\Lambda_b}^2(1-r+\hat{s})](|A_1|^2 - |B_1|^2) - 3[4m_\ell^2 - m_{\Lambda_b}^2(1-r+\hat{s})] \\
& \times(|D_1|^2 - |E_1|^2) - m_{\Lambda_b}^2(1-r-\hat{s})v^2(|A_1|^2 - |B_1|^2 + |D_1|^2 - |E_1|^2)\Big\} \\
& - \frac{1}{3}m_{\Lambda_b}^2\{12m_\ell^2(1-r) + m_{\Lambda_b}^2\hat{s}[3(1-r+\hat{s}) + v^2(1-r-\hat{s})]\}(|A_2|^2 - |B_2|^2) \\
& - \frac{2}{3}m_{\Lambda_b}^4\hat{s}(2-2r+\hat{s})v^2\,(|D_2|^2 - |E_2|^2)\Big\}\,,
\end{aligned} \tag{36}
$$

$$
\begin{aligned}
P_T(\hat{s}, m_{t\prime}, r_{sb}, \phi_{sb}) = & -\frac{8\pi m_{\Lambda_b}^3 v\sqrt{\hat{s}\lambda}}{\Delta(\hat{s}, m_{t\prime}, r_{sb}, \phi_{sb})}\Big\{ m_\ell\Big(\mathrm{Im}[(A_1 + B_1)^* F_1]\Big) \\
& - m_\ell m_{\Lambda_b}\Big[(1+\sqrt{r})\,\mathrm{Im}[(A_2 + B_2)^* F_1]\Big]
\end{aligned}
$$

$$+m_{\Lambda_b}^2(1-r+\hat{s})\Big(\mathrm{Im}[A_2^*D_1-A_1^*D_2]-\mathrm{Im}[B_2^*E_1-B_1^*E_2]\Big)$$
$$+2m_{\Lambda_b}\Big(\mathrm{Im}[A_1^*E_1-B_1^*D_1]-m_{\Lambda_b}^2\hat{s}\,\mathrm{Im}[A_2^*E_2-B_2^*D_2]\Big)\Big\}\,, \tag{37}$$

The dependence of the P_L, P_N and P_T polarizations of the Λ baryon on t' quark mass at $\hat{s}=0.5$ and at three fixed values of the r_{sb} and SM are shown in figures 6-11.

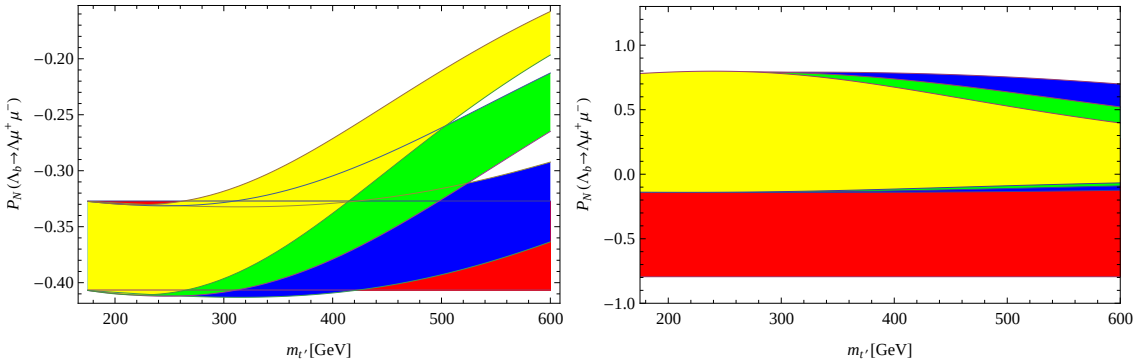

FIG. 6. The dependence of normal baryon polarization for the $\Lambda_b\to\Lambda\mu^+\mu^-$ decay on $m_{t'}$ at $\hat{s}=0.5$. The red band corresponds to the SM, while the blue, green and yellow bands belong to the SM4 for $r_{sb}=0.005,\ 0.01$ and 0.015, respectively. The left graph corresponds to the HQET while the graph on the right refers to the full QCD.

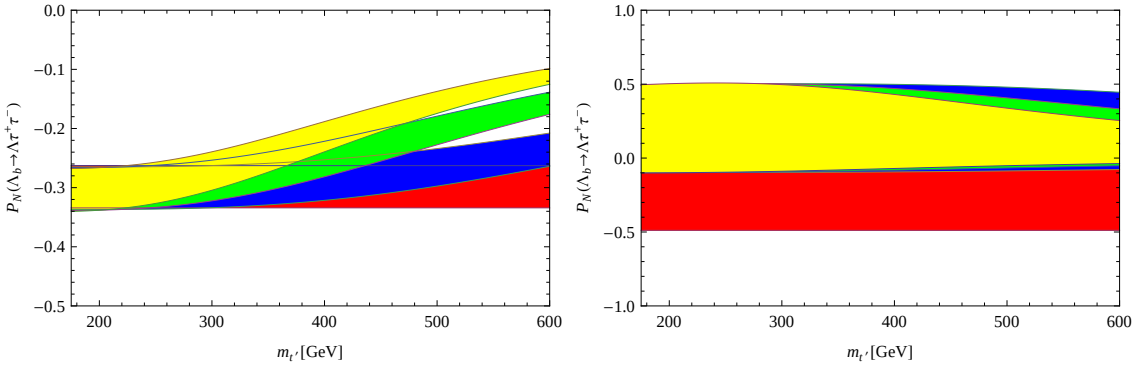

FIG. 7. The same as FIG. 6 but for τ.

A quick glance in the figures 6-11 leads to the following conclusions:

- The baryon polarizations also overall favor the $m_{t'}\simeq 400\ GeV$ for the lower limit of the fourth family quark.

- Our numerical analysis show that as far as the central values of the form factors are considered, there are considerable differences between the full theory predictions on the P_N and P_T and the HQET results for both lepton channels. This difference is small for the P_L and

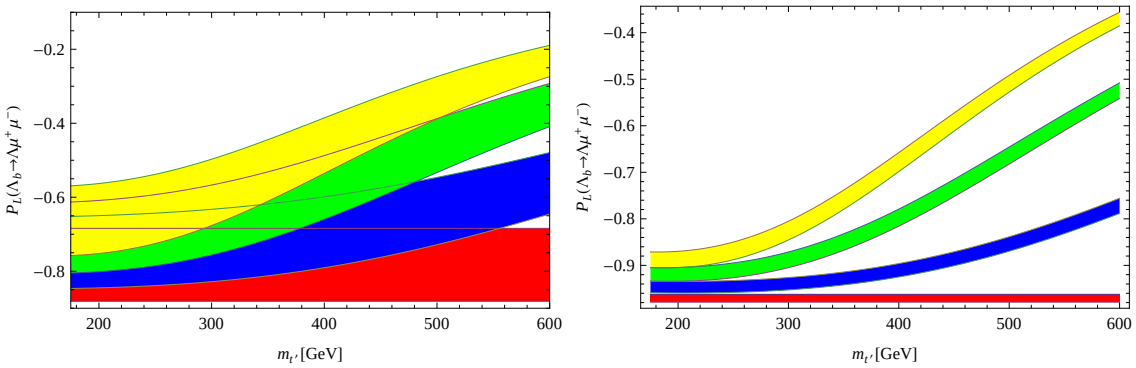

FIG. 8. The same as FIG. 5 but for longitudinal baryon polarization.

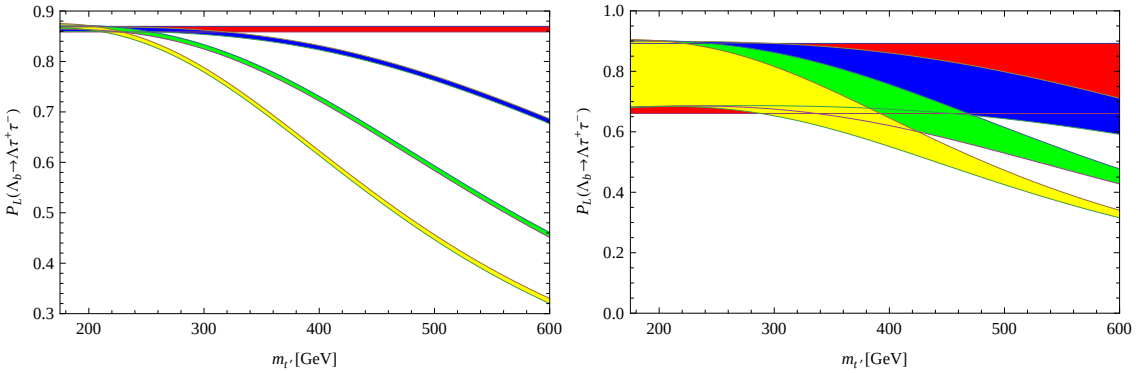

FIG. 9. The same as FIG. 8 but for τ.

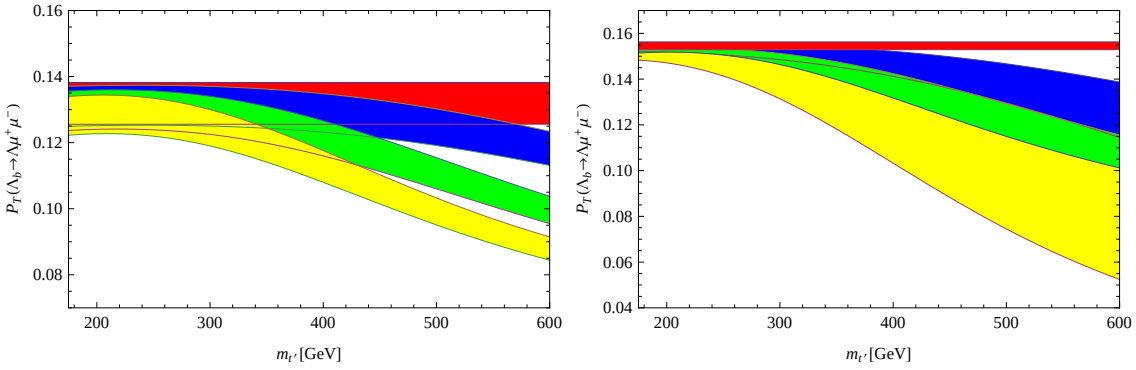

FIG. 10. The same as FIG. 5 but for transverse baryon polarization.

μ channel and is approximately zero for the longitudinal polarization and τ channel. When we consider the uncertainties of the form factors we detect sizable differences in both values and behavior of the baryon polarizations with respect to the $m_{t'}$ for all cases.

- Except the full QCD predictions on the P_N for both leptons and the P_T for the τ channel, the difference between the predictions of SM and SM4 grows with increasing the fourth generation quark mass. This difference also increases with increasing the value of the r_{sb}. In

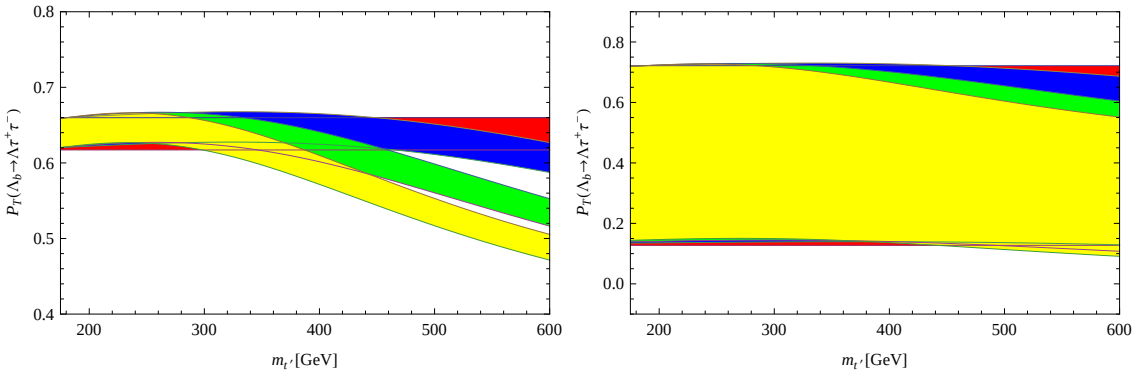

FIG. 11. The same as FIG. 10 but for τ.

the P_N for both leptons and the P_T for the τ channel, the uncertainties of the form factors lead to a very small difference between two model predictions.

- When we consider only the central values of the form factors, the $|P_N|$ in μ channel is larger than that of τ at any values of the fourth generation parameters. The situation is inverse in the case of $|P_T|$. The $|P_L|$ is approximately the same for both lepton channels.

D. Double Lepton Polarization Asymmetries

For the general model independent form of the effective Hamiltonian, the double lepton polarization asymmetries characterizing the considered decay channel are calculated in [28]. In the case of SM4, they reduce to the following explicit expressions in the rest frame of the $l^{\pm}$ (see also [29, 30]):

$$P_{LN}(\hat{s},m_{t'},r_{sb},\phi_{sb})=\frac{16\pi m_{\Lambda_b}^4\hat{m}_\ell\sqrt{\lambda}}{\Delta(\hat{s},m_{t'},r_{sb},\phi_{sb})\sqrt{\hat{s}}}\mathrm{Im}\Big\{(1-r)(A_1^*D_1+B_1^*E_1)+m_{\Lambda_b}\hat{s}(A_1^*E_3-A_2^*E_1$$
$$+B_1^*D_3-B_2^*D_1)+m_{\Lambda_b}\sqrt{r}\hat{s}(A_1^*D_3+A_2^*D_1+B_1^*E_3+B_2^*E_1)-m_{\Lambda_b}^2\hat{s}^2\Big(B_2^*E_3+A_2^*D_3\Big)\Big\}, \quad (38)$$

$$P_{LT}(\hat{s},m_{t'},r_{sb},\phi_{sb})=\frac{16\pi m_{\Lambda_b}^4\hat{m}_\ell\sqrt{\lambda}v}{\Delta(\hat{s},m_{t'},r_{sb},\phi_{sb})\sqrt{\hat{s}}}\mathrm{Re}\Big\{(1-r)\Big(|D_1|^2+|E_1|^2\Big)-\hat{s}\Big(A_1D_1^*-B_1E_1^*\Big)$$
$$-m_{\Lambda_b}\hat{s}\Big[B_1D_2^*+(A_2+D_2-D_3)E_1^*-A_1E_2^*-(B_2-E_2+E_3)D_1^*\Big]$$
$$+m_{\Lambda_b}\sqrt{r}\hat{s}\Big[A_1D_2^*+(A_2+D_2+D_3)D_1^*-B_1E_2^*-(B_2-E_2-E_3)E_1^*\Big]$$
$$+m_{\Lambda_b}^2\hat{s}(1-r)(A_2D_2^*-B_2E_2^*)-m_{\Lambda_b}^2\hat{s}^2(D_2D_3^*+E_2E_3^*)\Big\}, \quad (39)$$

$$P_{NT}(\hat{s},m_{t'},r_{sb},\phi_{sb})=\frac{64m_{\Lambda_b}^4\lambda v}{3\Delta(\hat{s},m_{t'},r_{sb},\phi_{sb})}\mathrm{Im}\Big\{(A_1D_1^*+B_1E_1^*)+m_{\Lambda_b}^2\hat{s}(A_2^*D_2+B_2^*E_2)\Big\}, \quad (40)$$

$$\begin{aligned}P_{NN}(\hat{s},m_{t'},r_{sb},\phi_{sb})=&\frac{32m_{\Lambda_b}^4}{3\hat{s}\Delta(\hat{s},m_{t'},r_{sb},\phi_{sb})}\mathrm{Re}\Big\{24\hat{m}_\ell^2\sqrt{r}\hat{s}(A_1B_1^*+D_1E_1^*)\\
&-12m_{\Lambda_b}\hat{m}_\ell^2\sqrt{r}\hat{s}(1-r+\hat{s})(A_1A_2^*+B_1B_2^*)\\
&+6m_{\Lambda_b}\hat{m}_\ell^2\hat{s}\Big[m_{\Lambda_b}\hat{s}(1+r-\hat{s})\Big(|D_3|^2+|E_3|^2\Big)+2\sqrt{r}(1-r+\hat{s})(D_1D_3^*+E_1E_3^*)\Big]\\
&+12m_{\Lambda_b}\hat{m}_\ell^2\hat{s}(1-r-\hat{s})(A_1B_2^*+A_2B_1^*+D_1E_3^*+D_3E_1^*)\\
&-[\lambda\hat{s}+2\hat{m}_\ell^2(1+r^2-2r+r\hat{s}+\hat{s}-2\hat{s}^2)]\Big(|A_1|^2+|B_1|^2-|D_1|^2-|E_1|^2\Big)\\
&+24m_{\Lambda_b}^2\hat{m}_\ell^2\sqrt{r}\hat{s}^2(A_2B_2^*+D_3E_3^*)-m_{\Lambda_b}^2\lambda\hat{s}^2v^2\Big(|D_2|^2+|E_2|^2\Big)\\
&+m_{\Lambda_b}^2\hat{s}\{\lambda\hat{s}-2\hat{m}_\ell^2[2(1+r^2)-\hat{s}(1+\hat{s})-r(4+\hat{s})]\}\Big(|A_2|^2+|B_2|^2\Big)\Big\}, \end{aligned} \quad (41)$$

$$\begin{aligned}P_{TT}(\hat{s},m_{t'},r_{sb},\phi_{sb})=&\frac{32m_{\Lambda_b}^4}{3\hat{s}\Delta(\hat{s},m_{t'},r_{sb},\phi_{sb})}\mathrm{Re}\Big\{-24\hat{m}_\ell^2\sqrt{r}\hat{s}(A_1B_1^*+D_1E_1^*)\\
&-12m_{\Lambda_b}\hat{m}_\ell^2\sqrt{r}\hat{s}(1-r+\hat{s})(D_1D_3^*+E_1E_3^*)-24m_{\Lambda_b}^2\hat{m}_\ell^2\sqrt{r}\hat{s}^2(A_2B_2^*+D_3E_3^*)\\
&-6m_{\Lambda_b}\hat{m}_\ell^2\hat{s}\Big[m_{\Lambda_b}\hat{s}(1+r-\hat{s})\Big(|D_3|^2+|E_3|^2\Big)-2\sqrt{r}(1-r+\hat{s})(A_1A_2^*+B_1B_2^*)\Big]\\
&-12m_{\Lambda_b}\hat{m}_\ell^2\hat{s}(1-r-\hat{s})(A_1B_2^*+A_2B_1^*+D_1E_3^*+D_3E_1^*)\\
&-[\lambda\hat{s}-2\hat{m}_\ell^2(1+r^2-2r+r\hat{s}+\hat{s}-2\hat{s}^2)]\Big(|A_1|^2+|B_1|^2\Big)\\
&+m_{\Lambda_b}^2\hat{s}\{\lambda\hat{s}+\hat{m}_\ell^2[4(1-r)^2-2\hat{s}(1+r)-2\hat{s}^2]\}\Big(|A_2|^2+|B_2|^2\Big)\\
&+\{\lambda\hat{s}-2\hat{m}_\ell^2[5(1-r)^2-7\hat{s}(1+r)+2\hat{s}^2]\}\Big(|D_1|^2+|E_1|^2\Big)\\
&-m_{\Lambda_b}^2\lambda\hat{s}^2v^2\Big(|D_2|^2+|E_2|^2\Big)\Big\}, \end{aligned} \quad (42)$$

$$\begin{aligned}P_{LL}(\hat{s},m_{t'},r_{sb},\phi_{sb})=&\frac{16m_{\Lambda_b}^4}{3\Delta(\hat{s},m_{t'},r_{sb},\phi_{sb})}\mathrm{Re}\Big\{\\
&-6m_{\Lambda_b}\sqrt{r}(1-r+\hat{s})\Big[\hat{s}(1+v^2)(A_1A_2^*+B_1B_2^*)-4\hat{m}_\ell^2(D_1D_3^*+E_1E_3^*)\Big]\\
&+6m_{\Lambda_b}(1-r-\hat{s})\Big[\hat{s}(1+v^2)(A_1B_2^*+A_2B_1^*)+4\hat{m}_\ell^2(D_1E_3^*+D_3E_1^*)\Big]\\
&+12\sqrt{r}\hat{s}(1+v^2)\Big(A_1B_1^*+D_1E_1^*+m_{\Lambda_b}^2\hat{s}A_2B_2^*\Big)\\
&+12m_{\Lambda_b}^2\hat{m}_\ell^2\hat{s}(1+r-\hat{s})\Big(|D_3|^2+|E_3^*|^2\Big)\\
&-(1+v^2)\Big[1+r^2-r(2-\hat{s})+\hat{s}(1-2\hat{s})\Big]\Big(|A_1|^2+|B_1|^2\Big)\\
&-\Big[(5v^2-3)(1-r)^2+4\hat{m}_\ell^2(1+r)+2\hat{s}(1+8\hat{m}_\ell^2+r)-4\hat{s}^2\Big]\Big(|D_1|^2+|E_1|^2\Big)\end{aligned}$$

$$
\begin{aligned}
&-m_{\Lambda_b}^2(1+v^2)\hat{s}\Big[2+2r^2-\hat{s}(1+\hat{s})-r(4+\hat{s})\Big]\big(\,|A_2|^2+|B_2|^2\,\big)\\
&-2m_{\Lambda_b}^2\hat{s}v^2\Big[2(1+r^2)-\hat{s}(1+\hat{s})-r(4+\hat{s})\Big]\big(\,|D_2|^2+|E_2|^2\,\big)\\
&+12m_{\Lambda_b}\hat{s}(1-r-\hat{s})v^2\Big(D_1E_2^*+D_2E_1^*\Big)\\
&-12m_{\Lambda_b}\sqrt{r}\hat{s}(1-r+\hat{s})v^2\Big(D_1D_2^*+E_1E_2^*\Big)\\
&+24m_{\Lambda_b}^2\sqrt{r}\hat{s}\Big(\hat{s}v^2D_2E_2^*+2\hat{m}_\ell^2D_3E_3^*\Big)\Big\},
\end{aligned}
\tag{43}
$$

where $\hat{m}_l=\frac{m_l}{m_{\Lambda_b}}$. Some of the double lepton polarization asymmetries as a function of the $m_{t'}$ at $\hat{s}=0.5$ and at three fixed values of the r_{sb} and the SM are shown in figures 12-21.

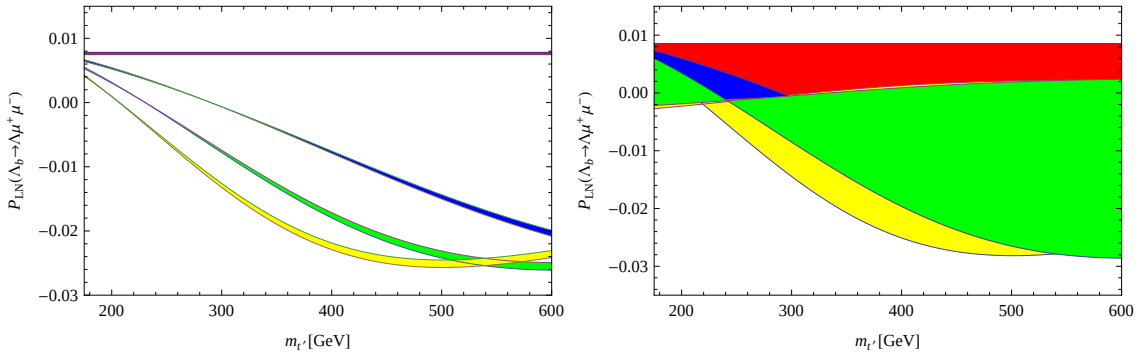

FIG. 12. The dependence of double lepton polarization asymmetry P_{LN} for the $\Lambda_b\to\Lambda\mu^+\mu^-$ decay on $m_{t'}$ at $\hat{s}=0.5$. The red band corresponds to the SM, while the blue, green and yellow bands belong to the SM4 for $r_{sb}=0.005,\ 0.01$ and 0.015, respectively. The left graph corresponds to the HQET while the graph on the right refers to the full QCD.

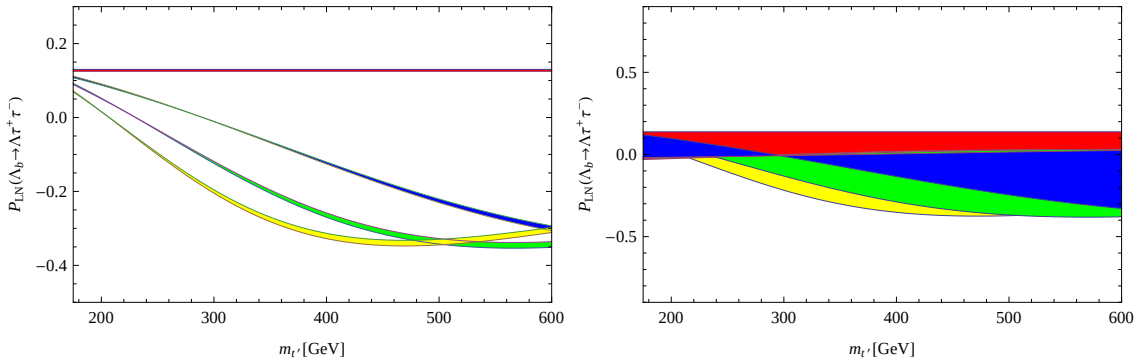

FIG. 13. The same as FIG. 12 but for τ.

From the analysis of the figures 12-21, we conclude the following items:

- When we consider only the central values of the form factors, our numerical results show that there are sizable differences between the full QCD and HQET results (HQET violation) in the P_{TT} and P_{NN} polarizations for τ channel and at fixed values of the fourth generation

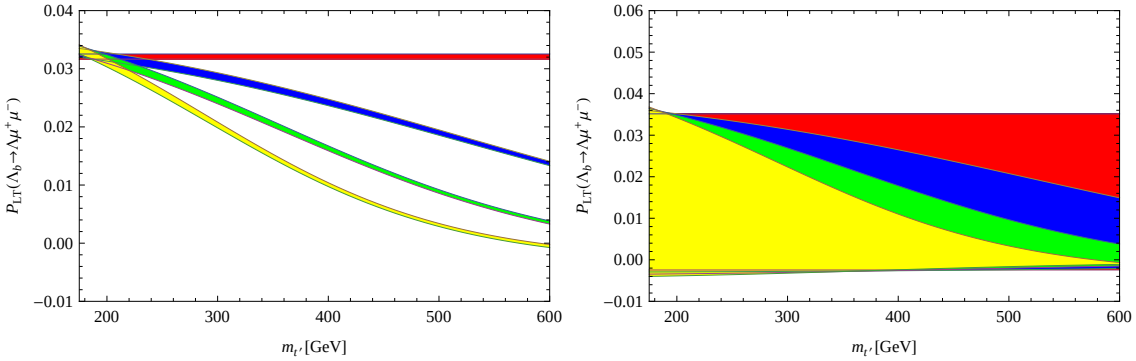

FIG. 14. The same as FIG. 12 but for P_{LT}.

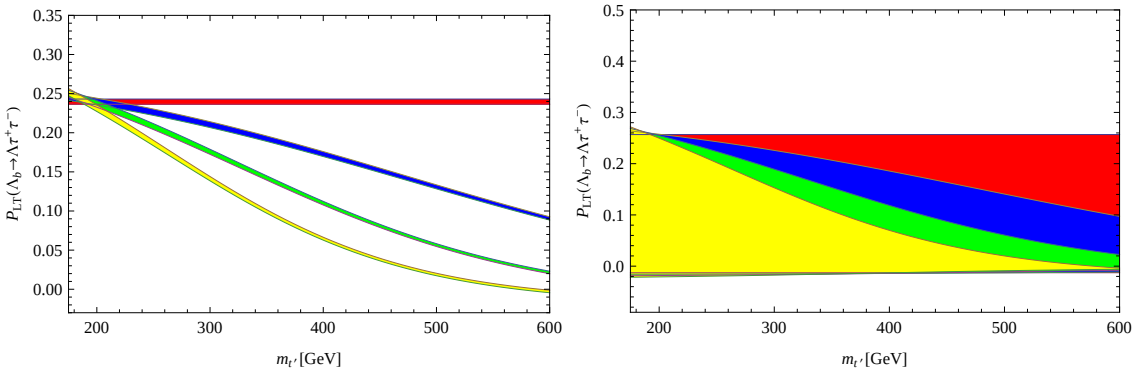

FIG. 15. The same as FIG. 14 but for τ.

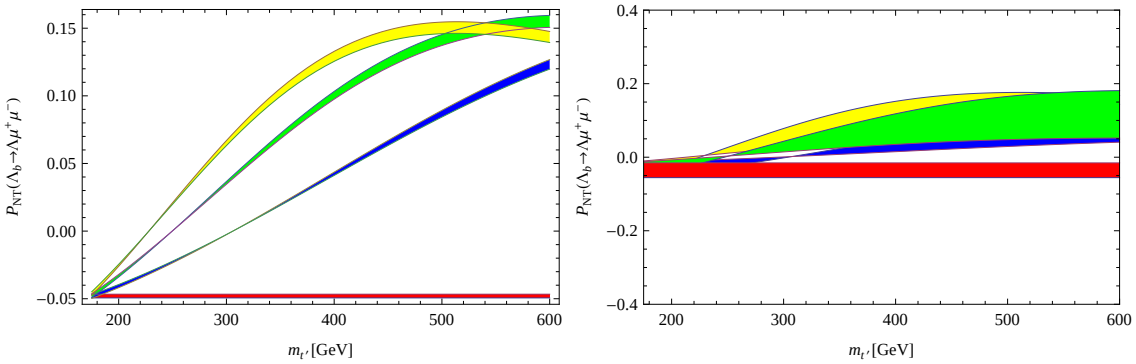

FIG. 16. The same as FIG. 12 but for P_{NT}.

parameters. The results of two models on P_{LT}, P_{LN} and P_{NT} for both leptons as well as the P_{NN} and P_{TT} for the μ channel deviate slightly from each other. When the uncertainties of the form factors are considered, we detect considerable differences between full QCD and the HQET models predictions on behavior of all double lepton polarization asymmetries with respect to the fourth family parameters.

- Comparing to the other physical quantities, the double lepton polarization asymmetries are

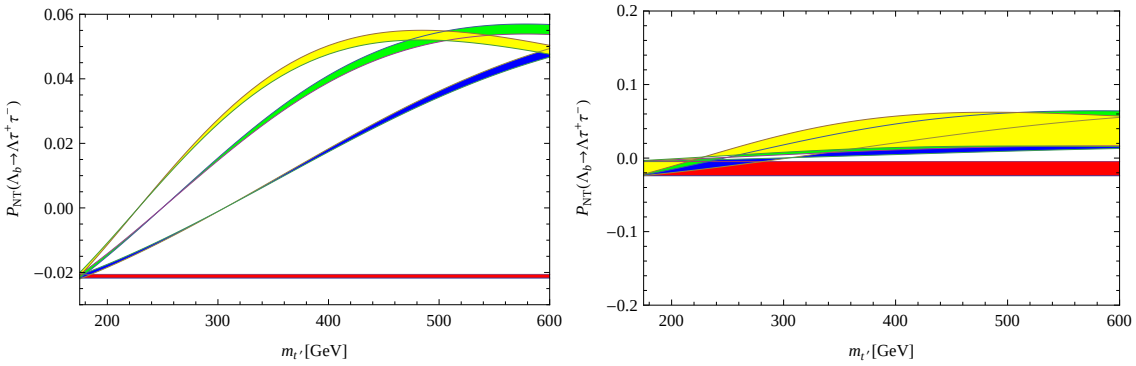

FIG. 17. The same as FIG. 16 but for τ.

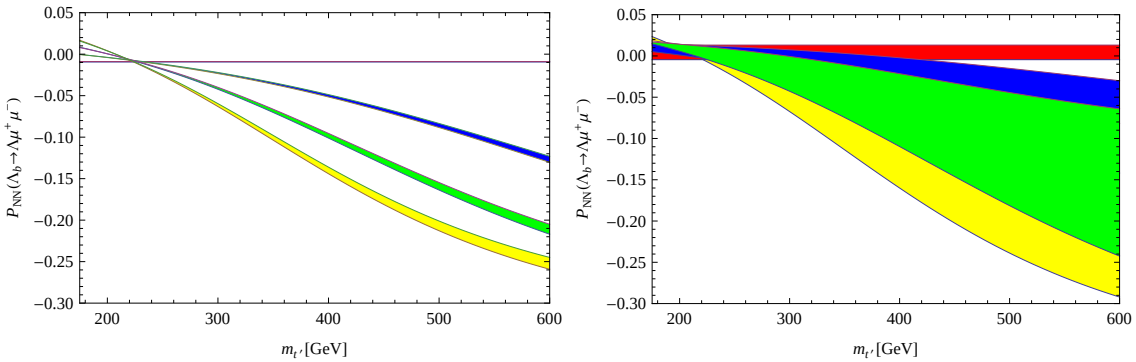

FIG. 18. The same as FIG. 12 but for P_{NN}.

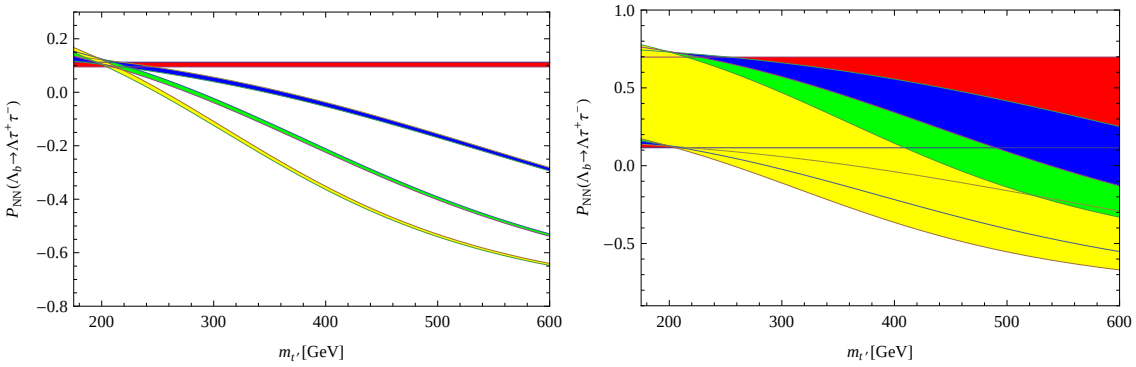

FIG. 19. The same as FIG. 18 but for τ.

more sensitive to the mass of the fourth generation quark at lower values of $m_{t'}$. This sensitivity is large in HQET compared to the full QCD such that starting from the $m_{t'} \simeq 200\ GeV$, we see sizable deviations of the SM4 results with those of the SM in HQET approaximation. However, in the full theory the discrepancy between the SM and SM4 results starts approaximately from $m_{t'} \simeq 300\ GeV$ and small compared to the HQET predictions.

- When we consider only the central values of the form factors, except than the P_{LN} and P_{NT}, the remaining double lepton polarization asymmetries grow increasing the $m_{t'}$ and

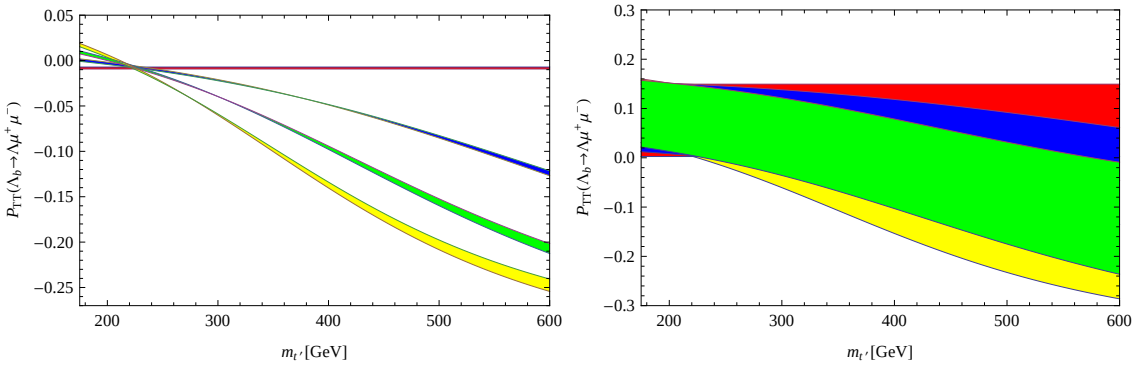

FIG. 20. The same as FIG. 12 but for P_{TT}.

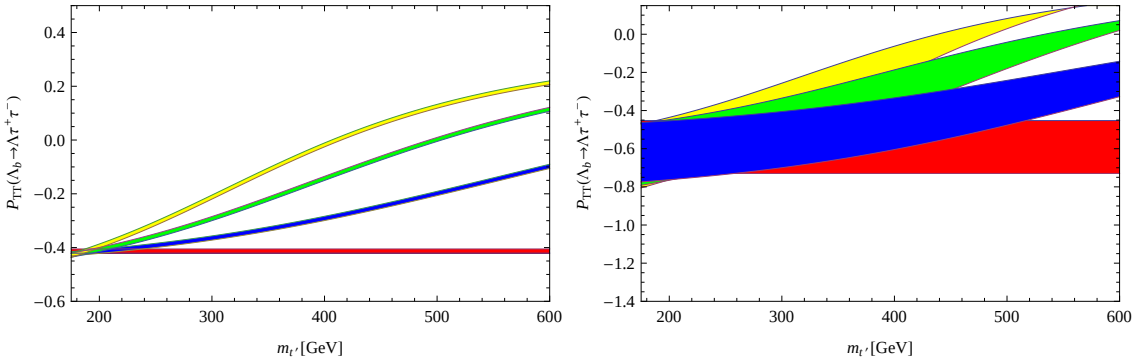

FIG. 21. The same as FIG. 20 but for τ.

value of the r_{sb}. For P_{LN} (P_{NT}), the maximum deviation belongs to the $r_{sb} = 0.015$ and $m_{t'} \simeq 450GeV$ ($r_{sb} = 0.010$ and upper bound of the $m_{t'}$).

IV. CONCLUSION

We have performed a comprehensive analysis on the $\Lambda_b \to \Lambda \ell^+ \ell^-$ transition both in the SM4 and SM models. In particular, using the form factors entering the low energy matrix elements both from full QCD as well as HQET, we have investigated the branching ratio, forward-backward asymmetry, double lepton polarization asymmetries and polarization of the Λ baryon. We have observed that there are overall sizable differences between the predictions of the SM and SM4 on the considered physical quantities when $m_{t'} \geq 400\ GeV$. This can be considered as an indication of the existence of the fourth family quarks should we search for in the future experiments. The results also depicted overall considerable differences between the predictions of the full QCD and those of the HQET. The orders of the branching ratios in both lepton channels show that these decay channels can be detected at LHCb. Any measurement on the considered physical quantities and their comparison with the theoretical predictions can give valuable information about both nature of the participating baryons and existence of the fourth family quarks.

[1] T. M. Aliev, K. Azizi, M. Savci, Phys. Rev. D 81, 056006 (2010).

[2] V. Bashiry, K. Azizi, JHEP 0707 (2007) 064 .

[3] F. Zolfagharpour, V. Bashiry, Nucl. Phys. B 796 (2008) 294.

[4] G. Turan, JHEP 0505 (2005) 008.

[5] A. J. Buras and M. Münz, Phys. Rev. D 52, 186 (1995).

[6] B. Grinstein, M. J. Savage and M. B. Wise, Nucl. Phys. B 319 (1989) 271.

[7] A. Soni, A. K. Alok, A. Giri, R. Mohanta, S. Nandi, Phys. Rev. D 82 (2010) 033009.

[8] B. Holdom et al., PMC Phys. A 3, 4 (2009).

[9] O. Eberhardt, A. Lenz, J. Rohrwild, Phys. Rev. D 82, 095006 (2010).

[10] M. Sahin, S. Sultansoy, S. Turkoz, Phys. Rev. D 83, 054022 (2011).

[11] A. J. Buras, M. Misiak, M. Münz and S. Pokorski, Nucl. Phys. B 424, 374 (1994).

[12] M. Misiak, Nucl. Phys. B 393, 23 (1993); Erratum ibid B 439, 161 (1995).

[13] T. M. Aliev, A. Ozpineci, M. Savci, Phys. Rev. D 65 (2002) 115002.

[14] T. Mannel, W. Roberts and Z. Ryzak, Nucl. Phys. B355 (1991) 38.

[15] C. S. Huang, H. G. Yan, Phys. Rev. D 59, 114022 (1999).

[16] T. M. Aliev, M. Savcı, Eur. Phys. J. C 50, 91 (2007).

[17] T. M. Aliev, A. Ozpineci, M. Savci, Nucl .Phys. B 649 (2003) 168.

[18] A. K. Giri, R. Mohanta, Eur. Phys. J. C 45, 151 (2006).

[19] S. Nandi, A. Soni, Phys. Rev. D 83, 114510 (2011).

[20] S. K. Garg, S. K. Vempati, Phys. Lett. B 702 (2011) 370.

[21] A. K. Alok, A. Dighe, D. London, Phys. Rev. D 83, 073008 (2011).

[22] H. Chen, W. Huo, arXiv:1101.4660 [hep-ph].

[23] W. S. Hou, H. L. Li, S. Mishima, M. Nagashima, Phys. Rev. Lett. 98, 131801 (2007).

[24] M. Junaid, M. J. Aslam, arXiv:1103.3934 [hep-ph].

[25] T. M. Aliev, A. Özpineci, M. Savcı, Phys. Rev. D 67, 035007 (2003).

[26] T. M. Aliev, A. Ozpineci, M. Savci, C. Yuce , Phys. Lett. B 542 (2002) 229.

[27] T. M. Aliev, A. Ozpineci, M. Savci, arXiv:hep-ph/0301019.

[28] T. M. Aliev, V. Bashiry, M. Savci, Eur. Phys. J. C 38 (2004) 283.

[29] T. M. Aliev, M. Savci, B. B. Sirvanli, Eur. Phys.J. C 52, 375 (2007).

[30] W. Bensalem, D. London, N. Sinha and R. Sinha, Phys. Rev. D 67, 034007 (2003).